Actinic flux determination from measurements of irradiance

A. Kylling,[1] A. R. Webb,[2] A. F. Bais,[3] M. Blumthaler,[4] R. Schmitt,[5] S. Thiel,[6]
A. Kazantzidis,[3] R. Kift,[2] M. Misslbeck,[6] B. Schallhart,[4] J. Schreder,[4]
C. Topaloglou,[3] S. Kazadzis,[3] and J. Rimmer[2]

Received 28 November 2002; revised 4 March 2003; accepted 2 May 2003; published 23 August 2003.

[1] The actinic flux describes the number of photons incident at a point, while the irradiance describes the radiant energy crossing a surface. An algorithm for conversion of irradiance to downwelling actinic flux has been developed and tested. The algorithm uses a simple method to distinguish between a cloudy and a cloudless sky. It is necessary to separate cloudy and cloudless situations, as the irradiance to actinic flux conversion depends on the radiance field which is rather different for cloudy and cloudless skies. Surface UV irradiance and downwelling actinic flux spectra were measured at five European locations which were representative of different climates. A total of 9015 synchronized actinic flux and irradiance spectra were available to test the proposed algorithm. The measured irradiance spectra were used to estimate downwelling actinic flux spectra. The estimated actinic flux spectra were compared with the measured actinic flux spectra for all cloud and aerosol situations encountered, a wide range of solar zenith angles, and surface conditions. The average ratio of the reproduced to measured downwelling actinic flux is 1.021 ± 0.085 in the UV-B and 1.015 ± 0.105 in the UV-A. In general, the performance of the algorithm is better at smaller solar zenith angles. *INDEX TERMS:* 0360 Atmospheric Composition and Structure: Transmission and scattering of radiation; 0365 Atmospheric Composition and Structure: Troposphere—composition and chemistry; 3359 Meteorology and Atmospheric Dynamics: Radiative processes; *KEYWORDS:* actinic flux, irradiance, UV, measurements, modeling

Citation: Kylling, A., et al., Actinic flux determination from measurements of irradiance, *J. Geophys. Res.*, *108*(D16), 4506, doi:10.1029/2002JD003236, 2003.

1. Introduction

[2] The actinic flux is the radiant quantity used to calculate various photodissociation rates that are used to describe the photochemistry of the atmosphere. It is also the relevant radiation quantity for many biological systems. It represents the total number of photons, or radiation, incident at a point [*Madronich*, 1987]. Instrumentation to measure the spectral actinic flux has become more common recently and has been used in a number of campaigns [*Hofzumahaus et al.*, 1999; *Müller et al.*, 1995; *Shetter and Müller*, 1999]. However, most UV monitoring stations measure the spectral irradiance, which is the radiant energy transported from all directions across a surface. A number of studies have investigated the relationship between the actinic flux and the irradiance [*Nader and White*, 1969; *Madronich*, 1987; *Ruggaber et al.*, 1993; *Van Weele et al.*, 1995; *Cotte et al.*, 1997; *Kazadzis et al.*, 2000; *McKenzie et al.*, 2002; *Webb et al.*, 2002a]. *Nader and White* [1969] reported regression results from actinic flux and irradiance measurements of integrated UV radiation (300–380 nm) made in Los Angeles. The differences between the actinic flux and the irradiance were elucidated in the paper by *Madronich* [1987]. Theoretical relationships between the actinic flux and the irradiance were presented by *Ruggaber et al.* [1993] and visualized by model radiative transfer calculations. *Van Weele et al.* [1995] compared measurements of the UV-A actinic flux, the UV-A irradiance, and the global radiation. Furthermore, they provided radiative transfer model investigations of the relationship between the actinic flux and the irradiance. While the earlier experimental studies used various broadband instruments, *Cotte et al.* [1997] utilized spectrally resolved measurements. They described an algorithm to convert from irradiance to photolysis rates and tested it against $J(O_3)$ and $J(NO_2)$ actinometer measurements. Furthermore, they provided extensive sensitivity studies of the ratio of the diffuse actinic flux to the diffuse irradiance. *Kazadzis et al.* [2000] retrieved downwelling UV actinic flux spectra from spectral measurements of the global and direct solar UV irradiance, while *McKenzie et al.*

[1]Norwegian Institute for Air Research, Kjeller, Norway.
[2]Department of Physics, University of Manchester Institute of Science and Technology, Manchester, UK.
[3]Physics Department, Laboratory of Atmospheric Physics, Aristotle University of Thessaloniki, Thessaloniki, Greece.
[4]Institute of Medical Physics, University of Innsbruck, Innsbruck, Austria.
[5]Meteorologie Consult GmbH, Kinogstein, Germany.
[6]Institut für Meteorologie und Klimaforschung, Karlsruhe GmbH, Garmisch Partenkirchen, Germany.

0148-0227/03/2002JD003236$09.00

[2002] investigated the relationship between photolysis rates derived from spectral measurements of actinic fluxes and irradiances during a campaign in Boulder, Colorado. Finally, *Webb et al.* [2002a] provided an empirical method to convert from UV spectral irradiance into spectral actinic fluxes and tested it on measurements from a campaign in Greece. In the present work, spectral measurements of the irradiance are used together with a new actinic flux to irradiance algorithm to estimate the downwelling actinic flux. The estimated downwelling actinic flux is compared against spectral actinic flux measurements made at different locations under all weather conditions.

[3] Relationships between the spectral actinic flux and the irradiance are useful if, for example, one would like to use existing UV irradiance data records to estimate the influence of variations in UV radiation on tropospheric chemistry or various biological systems. Obviously, measurements of the actinic flux are preferable, but actinic flux-irradiance relationships with associated uncertainties may yield valuable information otherwise not available.

[4] The present work is part of the Actinic flux determination from measurements of irradiance (ADMIRA) project. A 2 week measurement campaign was undertaken in August 2000 at Nea Michaniona, Greece [*Webb et al.*, 2002b]. The spectral actinic flux and irradiance were measured simultaneously with ancillary information describing the optical properties of the atmosphere. This was followed by a monitoring period where simultaneous measurements of the irradiance and the actinic flux were carried out at Garmisch-Partenkirchen, Germany; Innsbruck, Austria; Reading, England; and Thessaloniki, Greece. The monitoring started in late 2000 and went on throughout 2001, with the exception of periods lost due to instrument malfunction. Here the measurements are used together with an irradiance to actinic flux algorithm to quantify the accuracy with which the actinic flux may be derived from the irradiance.

[5] The paper is organized as follows: First, theoretical relationships between the actinic flux and the irradiance are presented together with an algorithm to connect the two and the identification of cloudy and cloudless skies discussed. Next, the algorithm is used to convert from irradiance to actinic flux, and the derived actinic fluxes are compared with the measured actinic fluxes. Finally, the results are discussed and summarized.

2. Theory

[6] The diffuse downward, $F_\downarrow$, and upward, $F_\uparrow$, actinic fluxes are defined as

$$F_\downarrow = \int_0^{2\pi} \int_0^{\pi/2} L(\theta,\phi)\sin\theta d\theta d\phi \quad (1)$$

$$F_\uparrow = \int_0^{2\pi} \int_{-\pi/2}^{0} L(\theta,\phi)\sin\theta d\theta d\phi, \quad (2)$$

where L is the radiance and θ and ϕ are the polar and azimuth angles, respectively [*Chandrasekhar*, 1960]. Similarly, the diffuse downward, $E_\downarrow$, and upward, $E_\uparrow$, irradiances are defined as

$$E_\downarrow = \int_0^{2\pi} \int_0^{\pi/2} L(\theta,\phi)\cos\theta\sin\theta d\theta d\phi \quad (3)$$

$$E_\uparrow = \int_0^{2\pi} \int_{-\pi/2}^{0} L(\theta,\phi)\cos\theta\sin\theta d\theta d\phi. \quad (4)$$

The direct irradiance E_0 is related to the direct actinic flux F_0 via $E_0 = \mu_0 F_0$, where μ_0 is the cosine of the solar zenith angle. The exact ratio of the actinic flux $F = F_0 + F_\downarrow + F_\uparrow$ to the total downward irradiance $E = E_0 + E_\downarrow$ is [*Ruggaber et al.*, 1993; *Van Weele et al.*, 1995]

$$\frac{F}{E} = \frac{F_\downarrow + F_\uparrow}{E_\downarrow} + \left(\frac{1}{\mu_0} - \frac{F_\downarrow + F_\uparrow}{E_\downarrow}\right)\frac{E_0}{E}. \quad (5)$$

By defining $F_\downarrow/E_\downarrow = \alpha$, $F_\uparrow/E_\uparrow = \beta$, and an albedo $A = E_\uparrow/E$, equation (5) may be written as

$$\frac{F}{E} = \alpha\left(1 + \frac{\beta}{\alpha}A\right) + \left(\frac{1}{\mu_0} - \alpha\right)\frac{E_0}{E}. \quad (6)$$

All parameters except μ_0 in equation (6) depend on the wavelength. The second term in the first parentheses is the contribution from the upwelling radiation. If the radiation quantity of interest is the downwelling actinic flux $F_d = F_0 + F_\downarrow$, equation (6) simplifies to

$$\frac{F_d}{E} = \alpha + \left(\frac{1}{\mu_0} - \alpha\right)\frac{E_0}{E}. \quad (7)$$

Note also that in the UV part of the spectrum, equation (7) is a good approximation to equation (6) for snow-free conditions, as the surface albedo is small in the UV.

[7] During ADMIRA, F_d and E were measured. Hence equation (7) will be used to convert from downwelling irradiance to the 2π downwelling actinic flux. For the conversion process the challenge is to obtain values for α and E_0/E that are representative for the radiance distribution when the irradiance measurement was made. Generally, both E_0/E and α depend on the wavelength, the solar zenith angle, the surface albedo, aerosol loading, and cloud amount. So, to quote *Ruggaber et al.* [1993]: "no simple expression for the diffuse ratio [α] can be given." Examples of modeled E_0/E and α for cloudless conditions are presented in Figures 1 and 2.

[8] The values of E_0/E and α are representative for the conditions encountered during the ADMIRA campaign in Greece for low aerosol loading (day 218, solid line in Figures 1 and 2) and high aerosol loading (day 223, dashed line in Figures 1 and 2). They are shown together with results for a pure Rayleigh scattering atmosphere (dotted line in Figures 1 and 2). On day 218 the aerosol optical depth at 350 nm was about 0.35 and on day 223 around 1.5. However, the aerosol optical depth varied throughout the day, leading to the small oscillations in the curves including aerosols. The results in Figures 1 and 2 were calculated using the UVSPEC radiative transfer model [*Mayer et al.*, 1997; *Kylling et al.*, 1998]. The ratio E_0/E decreases rapidly with increasing solar zenith angle. It is noted that E_0/E

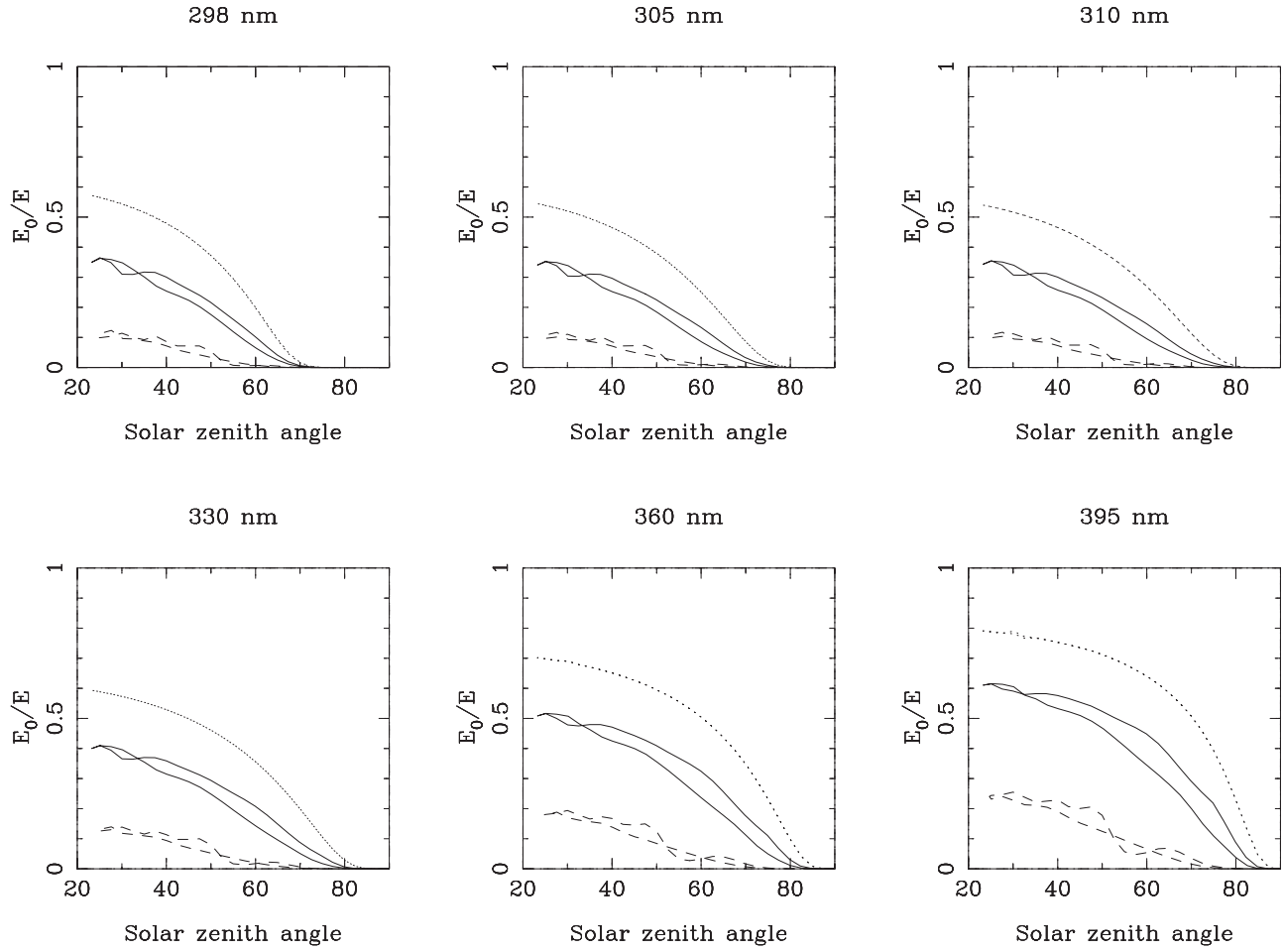

Figure 1. The modeled ratio of direct to total (= direct + diffuse) downward irradiance, E_0/E in equation (6), for days 218 (solid line) and 223 (dashed line), Nea Michaniona, Greece. For both days the afternoon ratios are larger than the morning ratios. The dotted line represents model calculations for a pure Rayleigh scattering sky; that is, no aerosols are included.

varies significantly with the aerosol load (solid line versus dashed line in Figure 1). The variations of α are largest at longer wavelengths and small aerosol loads where the direct beam contribution is largest (Figure 2). Hence to be able to estimate the actinic flux accurately from the irradiance under a cloudless sky, a lookup table approach was developed where E_0/E and α were tabulated as functions of aerosol optical depth, solar zenith angle, and wavelength. The variations of α with aerosol single-scattering albedo and phase function are insignificant compared to the variation with the aerosol optical depth [*Cotte et al.*, 1997].

[9] For an overcast sky, $E_0/E = 0$, and equation (7) reduces to

$$\frac{F_d}{E} = \alpha. \tag{8}$$

The variations of α with solar zenith angle for various surface albedos and wavelengths are shown in Figure 3.

[10] For a fixed surface albedo the variations of α are small with solar zenith angle. For a small-surface albedo of 0.07 representative for snow-free conditions, α varies between 1.72 and 1.74. As the albedo increases, α approaches the limit for isotropic diffuse scattering, $\alpha = 2$. The behavior of α is similar for all wavelengths where ozone absorption is negligible. However, where ozone absorption has an effect, the value of α is reduced as illustrated in Figure 3 for a surface albedo of 0.07. Changing the cloud height has minimal effect on α. For the conversion from irradiance to actinic flux performed here we take $\alpha = 1.73$ for overcast conditions for all wavelengths and solar zenith angles. This value is within the value of 1.70 ± 0.05 calculated by *Van Weele et al.* [1995] and the range of 1.75 ± 0.15 deduced from sky radiation distribution measurements by *Kazadzis et al.* [2000].

[11] To identify whether a measured spectrum is recorded under cloudy or cloudless conditions, a simple test was developed. The sky is identified as cloudless if

$$E_{\text{meas}} >= E_{\text{cloudless}} \times C \tag{9}$$

where $E_{\text{cloudless}}$ is the cloudless irradiance as estimated by the UVSPEC radiative transfer model. Furthermore, E_{meas} is the measured irradiance and C a tuning factor less than 1.0. The E_{meas} and $E_{\text{cloudless}}$ irradiances were calculated from measured and modeled spectra, respectively, as the sum of the irradiance between 350 and 365 nm. This

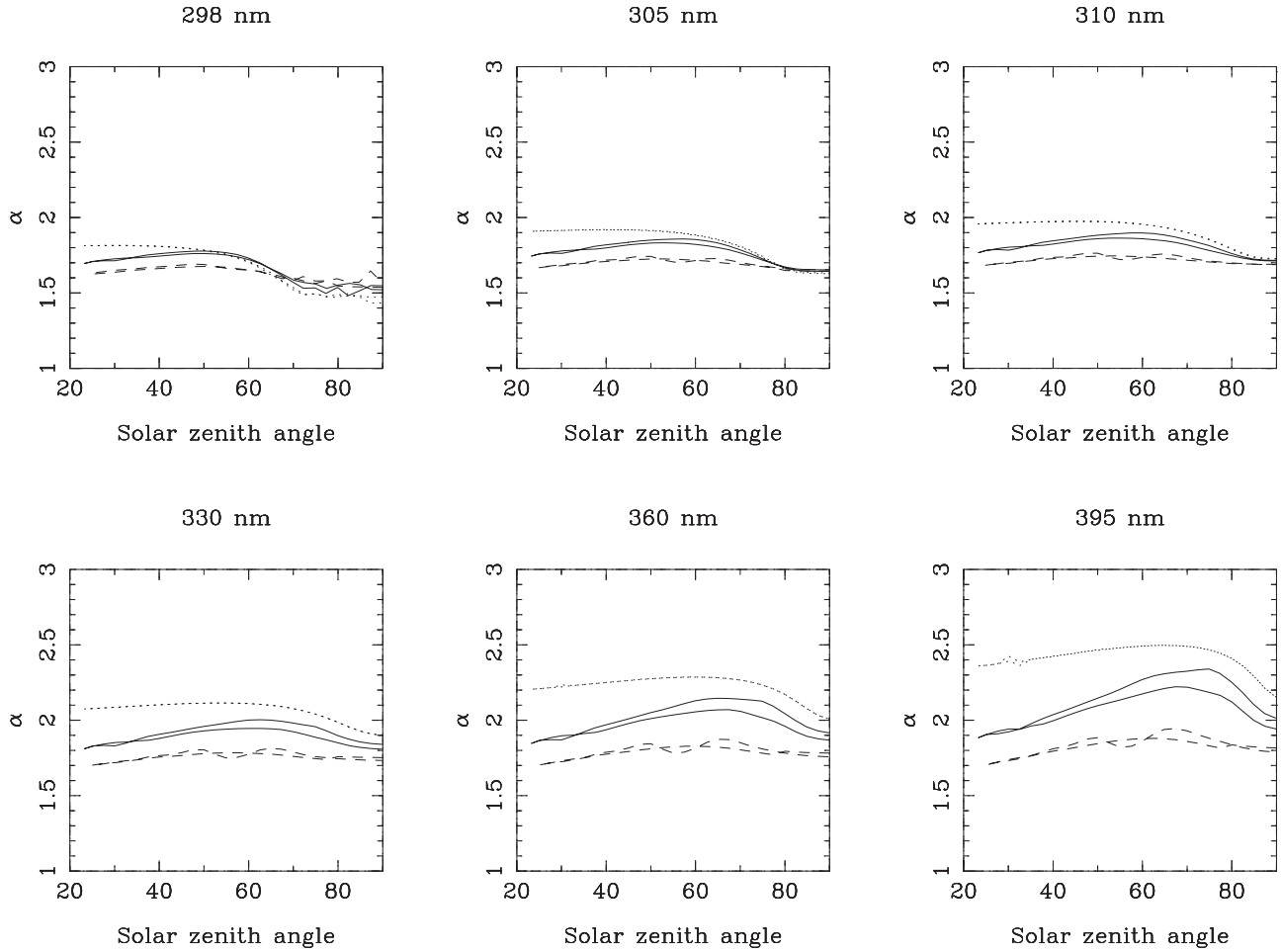

Figure 2. The modeled α in equation (9) for days 218 (solid line) and 223 (dashed line). The dotted line represents a pure Rayleigh scattering sky; that is, aerosols are not included.

wavelength choice was made because (1) it is preferable to work with a wavelength range where ozone does not absorb, (2) the longer the wavelength, the larger the direct beam contribution is to the total irradiance, (3) the upper limit had to be below the largest wavelength sampled by the various spectroradiometers, and (4) it is preferable to work with wavelength intervals instead of single wavelengths to avoid spurious measurement problems. The transmission defined as $E_{\text{meas}}/E_{\text{cloudless}}$ was used to determine the value of C. The frequency distribution of this transmission is shown in Figure 4 for all campaign and monitoring data described below.

[12] *McKenzie et al.* [2002] reported a bimodal frequency distribution for 4 days of data from Boulder, Colorado, and used a value of 0.8 to distinguish between cloudless and cloudy conditions. The distribution in Figure 4 has no clear bimodal shape, and thus various values of C were tried. A value of $C = 0.8$ was finally chosen since (1) it appears to identify most cloudless cases (Figure 4), (2) the corresponding reduction in the product $E_{\text{cloudless}} \times C$ is similar to the reduction achieved by adding a scatterer (cloud or aerosol) with an optical depth of 1.15 for a solar zenith angle of 30°, and hence the value of 0.8 includes both the effect of thin cirrus clouds and/or the presence of aerosols while excluding thick clouds, (3) the chosen value was successful in correctly identifying all spectra during the ADMIRA campaign as cloudless as stated below, and (4) a similar value was used in the study by *McKenzie et al.* [2002].

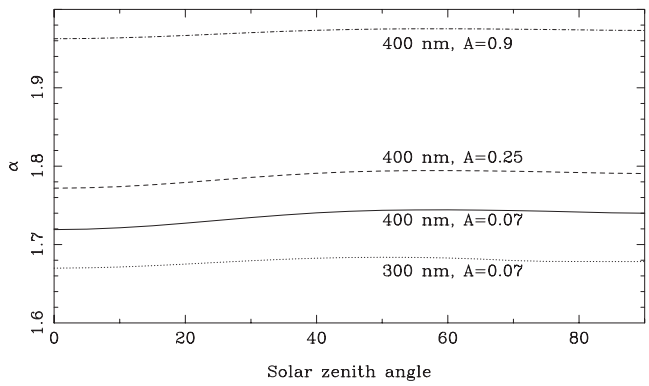

Figure 3. The α in equation (6) for an overcast sky as a function of solar zenith angle for various wavelengths and surface albedo conditions. The UVSPEC radiative transfer model was used to calculate α. The cloud used in the calculations was 2 km thick with the base at 8 km. The optical depth of the cloud was 15.

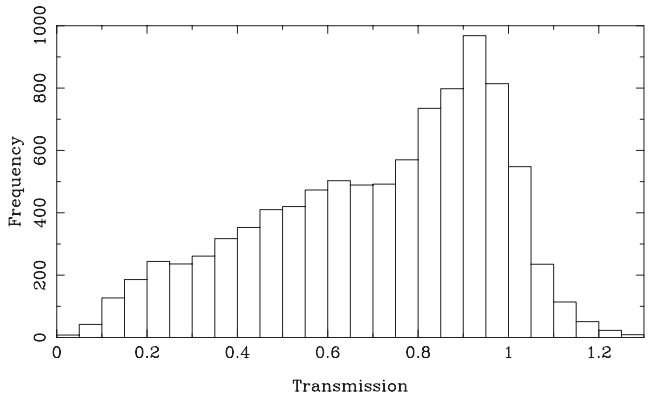

Figure 4. The frequency distribution of the transmission defined as $E_{meas}/E_{cloudless}$ where E_{meas} and $E_{cloudless}$ are derived from measured and modeled spectra, respectively, summed over the wavelength region 350–365 nm. All measurements during the campaign and monitoring parts of ADMIRA are included.

[13] Thus when the above condition, equation (9), is fulfilled and a cloudless situation is identified, equation (7) is employed to convert from irradiance to actinic flux. The lookup table with α and E_0/E as functions of wavelength, solar zenith angle, and aerosol optical depth is used to estimate the appropriate values of α and E_0/E needed for the conversion. Both α and E_0/E will vary with altitude. Thus while the method is general, the lookup table is site-specific. It is calculated using the UVSPEC radiative transfer model [*Mayer et al.*, 1997; *Kylling et al.*, 1998]. For situations identified as overcast, equation (8) was used with $\alpha = 1.73$.

3. Measurements and Results

[14] Two different measurement setups were used during ADMIRA. First, a 2 week intensive campaign was held in Greece. This was followed by long-term monitoring at the home sites of the various participants.

3.1. Campaign

[15] The aim of the ADMIRA campaign was to get a complete set of actinic flux, irradiance, direct irradiance, and radiance measurements together with ancilllary information such as aerosol extinction profiles, aerosol optical depth, ozone column, and ozone profiles. During the campaign held in August 2000, five spectroradiometers were located on a flat roof 30 m above sea level in a coastal complex at Nea Michaniona, Greece, 40.471°N, 22.848°E. The various spectroradiometers measured the actinic flux, the direct and global irradiances, and the radiance distribution. Details about the various spectroradiometers are provided by *Webb et al.* [2002b, and references therein]. Directly comparable measurements were performed by all instruments at intervals throughout the campaign to quantify the relative agreement. The results from these stability checks showed that the various measurements were equivalent on the 5% level. Further details on the stability checks and the measurement schedule have been described by *Webb et al.* [2002b]. During the campaign the sky was cloudless with variable amounts of aerosols. The aerosol optical depth varied from 0.4 to 0.5 at 350 nm for days of year 217–219 to up to 1.5 for days 222–223.

[16] Two Bentham DTM300 spectroradiometers measured either the irradiance or the actinic flux. When one was measuring the irradiance the other measured the actinic flux in synchronization and vice versa. The measured irradiance was used to estimate the actinic flux using equation (7) and the lookup table. The ratio of the estimated actinic flux integrated over the UV-B and the UV-A to the corresponding measured quantity is shown in Figure 5.

[17] As stated above, the sky was cloudless during the campaign, and the cloud detection method correctly identified all spectra as cloudless.

[18] For the data in Figure 5, available information on the total aerosol optical depth has been utilized to extract α and E_0/E from the lookup table. The average and the standard deviation of the estimated to measured actinic flux ratio are given in Table 1 (Nea Michaniona (all info)).

[19] If the aerosol information is not used the agreement in Table 1 between the estimated and the measured actinic flux deteriorates (Table 1, Nea Michaniona (standard)) and for large solar zenith angles and large aerosol optical depths differences may be up to 30% for individual cases. The estimated actinic fluxes are higher than those measured with the average estimated UV-A (UV-B) being 3.6 ± 2.8% (7.1 ± 4.3%) high. In general, the actinic fluxes estimated from the UMIST irradiances are larger than those estimated from IFU irradiances. This is consistent with the instrument comparison findings of *Webb et al.* [2002b], who suggest that the UMIST instrument is about 2% higher than the IFU instrument.

3.2. Monitoring

[20] During the monitoring phase the aim was to get actinic flux and irradiance data from various climatological regions for all kinds of weather situations. The four sites available were representative for Alpine, Mediterranean, and rural weather conditions. Calibration and quality control of the measured data were made at the individual measurement sites. For each site a lookup table was calculated as described above. Part of the motivation for the monitoring was to test the algorithm with no ancillary information available, a situation typically occurring at many stations. In this case, background aerosol conditions were assumed. Thus the aerosol optical depth was set to 0.1 at 350 nm for Innsbruck, Reading, and Garmisch-Partenkirchen and to 0.2 at 350 nm for Thessaloniki. The wavelength dependence was described using the Ångström formula with Ångström α equal to 1.3. Below the actinic flux as derived from the irradiance measurements are compared with simultaneous actinic flux measurements.

3.2.1. Innsbruck, Austria

[21] At the roof of the Institute of Medical Physics, University of Innsbruck, Austria (47.262°N, 11.380°E, elevation 577 m), the irradiance and the actinic flux were measured by a Bentham DTM300. A split fibre and shutters were used to select either the irradiance or the actinic flux input optics. For each wavelength, first the irradiance is recorded and next the actinic flux. Hence for each individual point in a spectrum the irradiance and actinic flux are measured as simultaneously in time as possible with a

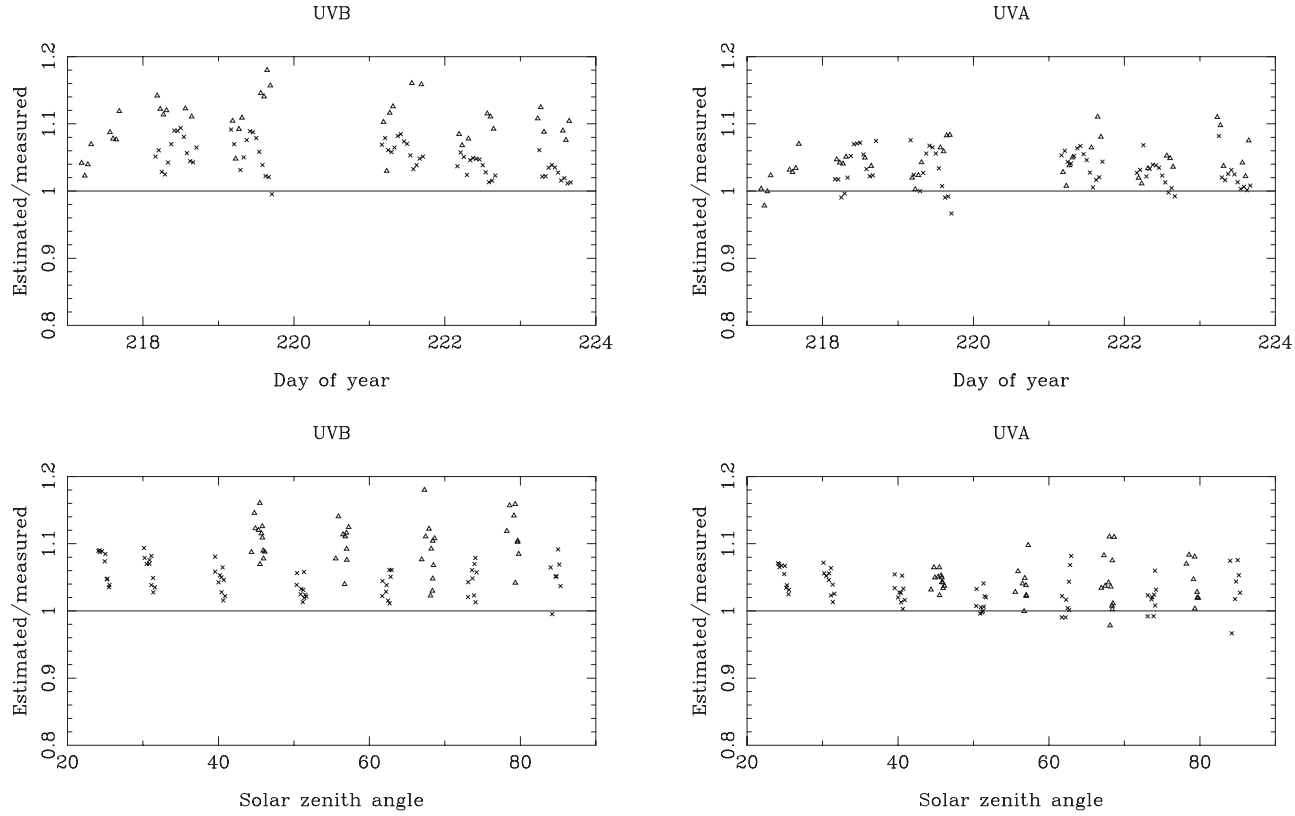

Figure 5. Ratio of the estimated actinic flux to the measured actinic flux for the Actinic flux determination from measurements of irradiance (ADMIRA) campaign held in Nea Michaniona, Greece, August 2000. (left) Ratios of UV-B (280–320 nm) as a function of day of year (top left) and solar zenith angle (bottom left). (right) Same, but for UV-A (320–400 nm). The open triangles denote ratios using the University of Manchester Institute of Science and Technology (UMIST) spectroradiometer irradiance to estimate the actinic flux to the actinic flux measured by the Fraunhofer Institute for Atmospheric Research (IFU) spectroradiometer. Crosses denote ratios using IFU irradiances and UMIST actinic fluxes.

scanning spectroradiometer. Data are available from the end of 2000 throughout most of 2001. The ratios of the estimated to the measured actinic flux integrated over the UV-B and UV-A for the Innsbruck site are shown in Figure 6.

[22] The UV-B and UV-A ratios are shown as function of day of year and solar zenith angle. The open triangles in Figure 6 denote cases identified as cloudless while crosses denote cloudy cases. On the average the estimated UV-A and UV-B actinic fluxes are 4% higher than the corresponding measured actinic fluxes (Table 1). The horizon of the Innsbruck site is formed by mountains which occupy 18% of the sky. This reduces the diffuse actinic flux compared to a location with no obstacles on the horizon. Thus the 4% higher estimated actinic flux may in part be explained by the measured actinic flux being low due to horizon effects. The standard deviation is higher for UV-A than UV-B. This is also evident in Figure 6, where the spread of the ratio is larger for UV-A than UV-B. As α varies more with the solar zenith angle at longer wavelengths compared to shorter wavelengths for a cloudless sky (see Figure 2), the conversion is more sensitive to α at longer wavelengths.

[23] In cases where the estimated actinic flux is clearly too large, the situation has always been identified as cloudless and vice versa, i.e., when the estimated actinic flux is too low that case has always been identified as cloudy. Misidentification may typically happen during broken cloud situations. However, no on-site information is available on cloud cover.

Table 1. The Average and Standard Deviation of the UV-B and UV-A Estimated to Measured Actinic Flux Ratios in Figures 6–8 and the Percentage of Cases Identified as Cloudy[a]

	UVB (280–320 nm)		UVA[b] (320–400 nm)			
Station	Average	Standard Deviation	Average	Standard Deviation	Cloudy, %	Number of Cases
Campaign						
Nea Michaniona, all info	1.071	0.043	1.036	0.028		106
Nea Michaniona, standard	1.077	0.067	1.040	0.107		106
Monitoring						
Innsbruck	1.040	0.053	1.041	0.102	49.9	4177
Reading	1.005	0.089	0.999	0.102	63.6	3329
Thessaloniki	1.000	0.079	1.000	0.095	49.5	1403
Garmisch-Partenkirchen	1.413	0.888	1.360	0.897	76.1	775

[a]Number of cases are the total number of simultaneous irradiance and actinic flux spectra available for each location.
[b]For Thessaloniki the upper limit is 365 nm.

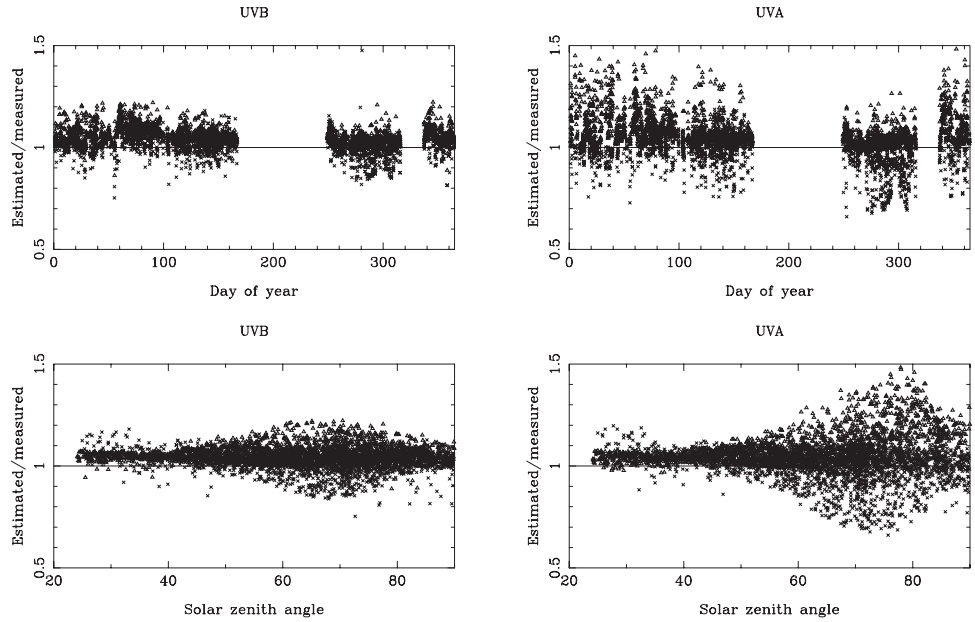

Figure 6. Ratio of the deduced actinic flux to the measured actinic flux for the site in Innsbruck. The data for days 320 and larger are from 2000 while the rest are from 2001. (left) Ratios of UV-B (280–320 nm) as a function of day of year (top left) and solar zenith angle (bottom left). (right) Same, but for UV-A (320–400 nm). Cases identified as cloudless are denoted by open triangles while cloudy cases are denoted by crosses.

3.2.2. Reading, England

[24] In Reading (51.450°N, −0.930°E, elevation 66 m), two scanning spectroradiometers were colocated. One, Bentham DTM150, measured the irradiance and the other, Bentham DTM300, the actinic flux. The two instruments were synchronized. Data are available between end of March 2001 until end of June 2001. The estimated/measured actinic flux ratios for Reading are shown in Figure 7.

[25] The average agreements between the measured and estimated actinic fluxes are good, but the standard deviation is somewhat larger than for the Innsbruck and Thessaloniki sites (Table 1). This larger spread may be attributed to synchronization problems between the two spectroradiometers.

3.2.3. Thessaloniki, Greece

[26] On the roof of the Physics Department, Laboratory of Atmospheric Physics, Aristotle University of Thessaloniki, Greece (40.517°N, 22.967°E, elevation 60 m), the irradiance was measured by a Brewer Mark III and the actinic flux by a CVI laser. Both are double monochromators with photomultiplier tube detectors. The measurements were synchronized in time, and data are available for most of 2001.

[27] The data for the site in Thessaloniki are presented in Figure 8.

[28] The differences between UV-A and UV-B are smaller than for the other sites. This is due to the UV-A measurements covering the smaller range 320–365 nm at the Thessaloniki site. The spread in the ratio is fairly constant with solar zenith angle as opposed to the data from the Innsbruck site (Figure 6). This may be due to the presence of a more hazy maritime atmosphere in Thessaloniki compared to the alpine site in Innsbruck.

3.2.4. Garmisch-Partenkirchen, Germany

[29] At the Institut für Meteorologie und Klimaforschung, Garmisch-Partenkirchen, Germany (47.480°N, 11.070°E, elevation 730 m), a Bentham DTM300 measured the irradiance and the actinic flux using a split fibre and shutters to choose between the two entrance optics. The experimental setup meant an irradiance spectrum was measured first, followed by an actinic flux spectrum. This means that the irradiance and actinic flux spectra are separated in time by 15–20 min. Thus the actinic flux spectra may have been recorded under different cloud conditions than the irradiance spectra used to derive the actinic flux. Furthermore, a time difference of 15–20 min causes significant differences in the solar zenith angles between the irradiance and the actinic flux spectra. Owing to lack of synchronization, the ratio of estimated to measured actinic flux deviates significantly from 1 (see Table 1).

4. Discussion and Conclusions

[30] An algorithm to estimate a downwelling actinic flux spectrum from a measured irradiance spectrum has been developed. The algorithm involves two steps. First, the irradiance spectrum is checked to determine whether it was recorded during cloudless or cloudy conditions. This is done by comparing the measured irradiance with a model-calculated cloudless irradiance. If the measured irradiance is less than the cloudless model irradiance times a threshold, the measured spectrum is identified as cloudy. Second, the irradiance is converted to actinic flux using equation (7) for cloudless and equation (8) for cloudy conditions.

[31] The algorithm has been applied to irradiance data gathered during a comprehensive measurement campaign

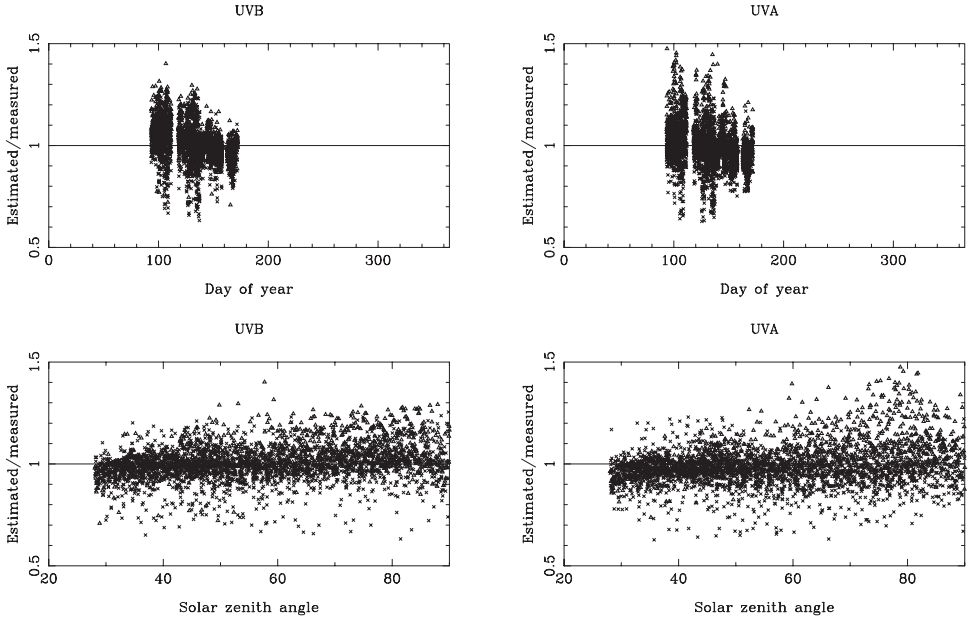

Figure 7. Similar to Figure 6, but for the site in Reading. The data are all from 2001.

under cloudless conditions in Greece. The estimated actinic fluxes are larger than the measured actinic fluxes by 7.1 ± 4.3% in the UV-B and 3.6 ± 2.8% in the UV-A. Part of this offset is due to differences in calibration between the instruments used to perform the irradiance and actinic flux measurements.

[32] Aerosol optical depth information was available for the campaign. Not utilizing the aerosol optical depth information during the conversion makes the agreement worse and especially so for large solar zenith angles and long wavelengths where the difference for individual cases may be up to 30%.

[33] The estimated actinic flux spectra may be used to calculate various photodissociation rates if the ambient temperature is known. For the campaign the $J(O_3)$ and $J(NO_2)$ photodissocation frequencies

$$O_3 + h\nu \rightarrow O_2 + O(^1D) \tag{10}$$

$$NO_2 + h\nu \rightarrow NO + O \tag{11}$$

were calculated using the estimated actinic fluxes and the measured actinic fluxes. The ratios of the two are shown in Figure 9.

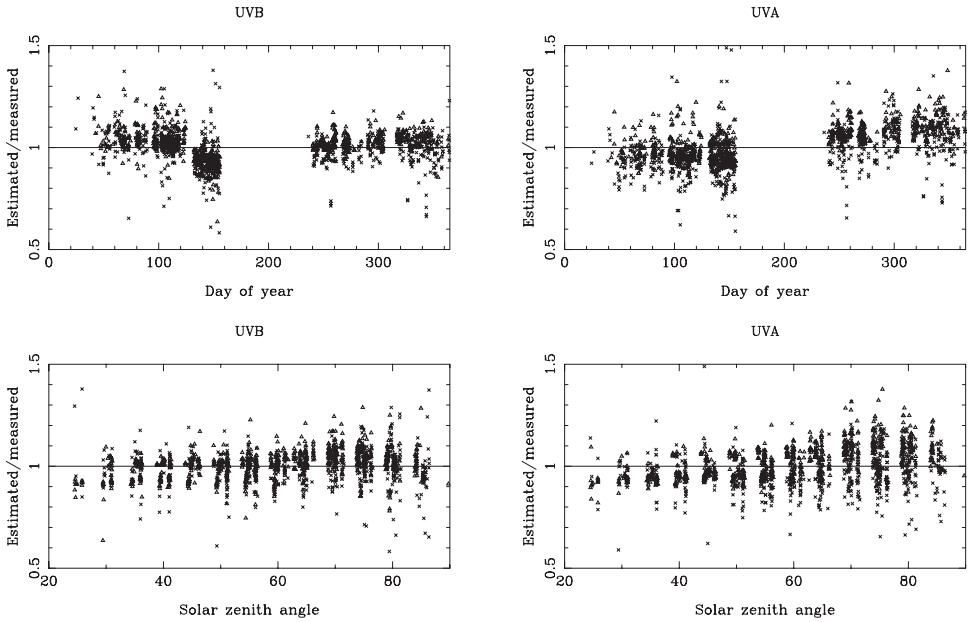

Figure 8. Similar to Figure 6, but for the site in Thessaloniki. The data are all from 2001. UV-A here covers the range 320–365 nm.

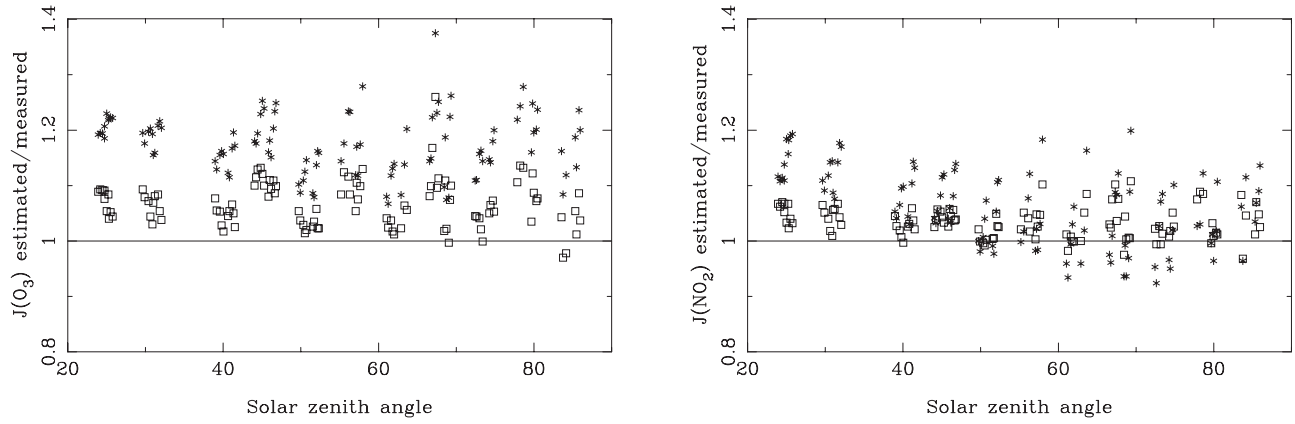

Figure 9. The ratio of the estimated and measured $J(O_3)$ and $J(NO_2)$ photodissocation frequencies with α and E_0/E from lookup tables (open squares). Also shown is the same ratio but using the isotropic assumption for the diffuse downwelling radiation, e.g., $\alpha = 2.0$ (asterisks).

[34] Also shown in Figure 9 are the same ratios but with the estimated actinic flux calculated assuming isotropic diffuse radiation ($\alpha = 2$ in equation (7). It is clearly seen that the assumption that the diffuse radiation is isotropic does not provide a satisfactory description of the radiance distribution and that it overestimates the actinic flux, particularly for $J(O_3)$. For $J(NO_2)$ the overestimate decreases with increasing solar zenith angle. This is in agreement with the findings of *Kazadzis et al.* [2000].

[35] The algorithm has also been applied to colocated and simultaneous measurements of the spectral irradiance and actinic flux at four sites in Europe. The measurements were made under all kinds of weather situations, and the sites represented different climatological regions. The estimated actinic flux has been compared to the measured actinic flux. For synchronized irradiance and actinic flux spectra the average of the reproduced to measured actinic flux varies between 0.999 and 1.077 (Table 1), with standard deviations of 10% or less. In general, the performance of the algorithm improves with decreasing solar zenith angle. Also, the standard deviation tends to be smaller for UV-B than UV-A. Thus photodissociation rates for processes that dissociate mostly in the presence of short-wavelength UV radiation such as $J(O^1D)$ may be more accurately estimated from irradiance measurements than processes that are more sensitive to longer wavelengths such as the photodissociation of nitrogen dioxide, $J(NO_2)$.

[36] Some of the sites have snow in the wintertime. However, the effective surface albedo for the sites will still be relatively low, 0.3, owing to the presence of trees, roads, and buildings. For an effective surface albedo of 0.3 the α in equation (7) increases by 5%. To estimate the total actinic flux, equation (7) should be used. Assuming a Lambert reflecting surface for which $\beta = 2$, it is straightforward to estimate F.

[37] Finally, it is noted that for all sites more than half of all irradiance spectra were identified as cloudy by the method presented in section 2, except for the site in Garmisch-Partenkirchen (Table 1). However, for Garmisch-Partenkirchen the time period covered may be too short to be representative. For a 2 year study of UV data from Potsdam, Germany, *Feister and Gericke* [1999] found that a total of 5% of spectra were recorded under clear sky. The present cloud detection method most likely significantly overestimates the number of cloudless situations. More sophisticated automatic cloud detection methods also have the same tendency [*Duchon and O'Malley*, 1999]. This is most likely due to situations involving broken and cirrus clouds. Broken clouds are especially difficult to identify with the present method which is weighted toward clouds crossing the Sun's path.

[38] Methods, such as the one presented here, to convert from irradiance to actinic flux may be used on existing irradiance data sets to gain insight into photochemistry, the response of various biological systems to radiation, and other applications where the actinic flux is the relevant radiation quantity. However, despite the possibility of using such algorithms, we strongly recommend that if the actinic flux is the primary radiation quantity of interest, it should be measured in preference to the irradiance. The irradiance to actinic flux algorithm, including calculation of lookup tables, is part of the Libradtran software package, which is available at http://www.libradtran.org.

[39] **Acknowledgments.** This work was done within the framework of the ADMIRA project funded by the European Commission (contract EVK2-1999-00167).

References

Chandrasekhar, S., *Radiative Transfer*, Dover, Mineola, N. Y., 1960.

Cotte, H., C. Devaux, and P. Carlier, Transformation of irradiance measurements into spectral actinic flux for photolysis rates determination, *J. Atmos. Chem.*, *26*, 1–28, 1997.

Duchon, C. E., and M. S. O'Malley, Estimating cloud type from pyranometer observations, *J. Appl. Meteorol.*, *38*, 132–141, 1999.

Feister, U., and K. Gericke, Cloud flagging of UV spectral irradiance measurements, *Atmos. Res.*, *49*, 115–138, 1999.

Hofzumahaus, A., A. Kraus, and M. Müller, Solar actinic flux spectroradiometry: A technique for measuring photolysis frequencies in the atmosphere, *Appl. Opt.*, *38*, 4443–4460, 1999.

Kazadzis, S., A. F. Bais, D. Balis, C. S. Zerefos, and M. Blumthaler, Retrieval of downwelling UV actinic flux density spectra from spectral measurements of global and direct solar UV irradiance, *J. Geophys. Res.*, *105*, 4857–4864, 2000.

Kylling, A., A. F. Bais, M. Blumthaler, J. Schreder, C. S. Zerefos, and E. Kosmidis, The effect of aerosols on solar UV irradiances during the Photochemical Activity and Solar Ultraviolet Radiation campaign, *J. Geophys. Res.*, *103*, 26,051–26,060, 1998.

Madronich, S., Photodissociation in the atmosphere: 1. Actinic flux and the effects of ground reflections and clouds, *J. Geophys. Res.*, *92*, 9740–9752, 1987.

Mayer, B., G. Seckmeyer, and A. Kylling, Systematic long-term comparison of spectral UV measurements and UVSPEC modeling results, *J. Geophys. Res.*, *102*, 8755–8767, 1997.

McKenzie, R., P. Johnston, A. Hofzumahaus, A. Kraus, S. Madronich, C. Cantrell, J. Calvert, and R. Shetter, Relationship between photolysis frequencies derived from spectroscopic measurements of actinic fluxes and irradiances during the IPMMI campaign, *J. Geophys. Res.*, *107*(D5), 4042, doi:10.1029/2001JD000601, 2002.

Müller, M., A. Kraus, and A. Hofzumahaus, $O_3 \rightarrow O(^1D)$ photolysis frequencies determined from spectroradiometric measurements of solar actinic UV radiation: Comparison with chemical actinometer measurements, *Geophys. Res. Lett.*, *22*, 679–682, 1995.

Nader, J. S., and N. White, Volumetric measurement of ultraviolet energy in urban atmosphere, *Environ. Sci. Technol.*, *3*, 848–854, 1969.

Ruggaber, A., R. Forkel, and R. Dlugi, Spectral actinic flux and its ratio to spectral irradiance by radiation transfer calculations, *J. Geophys. Res.*, *98*, 1151–1162, 1993.

Shetter, R. E., and M. Müller, Photolysis frequency measurements using actinic flux spectroradiometry during the PEM-Tropics mission: Instrumentation description and some results, *J. Geophys. Res.*, *104*, 5647–5661, 1999.

Van Weele, M., J. V.-G. de Arleeano, and F. Kuik, Combined measurements of UV-A actinic flux, UV-A irradiance and global radiation in relation to photodissociation rates, *Tellus, Ser. B*, *47*, 333–364, 1995.

Webb, A. R., R. Kift, S. Thiel, and M. Blumthaler, An empirical method for the conversion of spectral UV irradiance measurements to actinic flux data, *Atmos. Environ.*, *36*, 4044–4397, 2002a.

Webb, A. R., et al., Measuring spectral actinic flux and irradiance: Experimental results from the ADMIRA (Actinic Flux Determination from Measurements of Irradiance), *J. Atmos. Oceanic Technol.*, *19*, 1049–1062, 2002b.

A. F. Bais, S. Kazadzis, A. Kazantzidis, and C. Topaloglou, Laboratory of Atmospheric Physics, Physics Department, Aristotle University of Thessaloniki, 540 06 Thessaloniki, Greece. (abais@ccf.auth.gr; skaza@ccf.auth.gr; akaza@ccf.auth.gr; ctopa@ccf.auth.gr)

M. Blumthaler, B. Schallhart, and J. Schreder, Institute of Medical Physics, Müllerstrasse 44, A-6020 Innsbruck, Austria. (Mario.Blumthaler@uibk.ac.at; barbara.schallhart@uibk.ac.at; Josef.Schreder@uibk.ac.at)

R. Kift, J. Rimmer, and A. Webb, Department of Physics, University of Manchester Institute of Science and Technology, P.O. Box 88, Manchester M60 1QD, UK. (richard.kift@umist.ac.uk; john.rimmer@umist.ac.uk; ann.webb@umist.ac.uk)

A. Kylling, Norwegian Institute for Air Research, N-2027 Kjeller, Norway. (arve.kylling@nilu.no)

M. Misslbeck and S. Thiel, Institut für Meteorologie und Klimaforschung, Bereich Atmosphaerische Umweltforschung, Forschungszentrum Karlsruhe GmbH, Kreuzeckbahnstrasse 19, D-82467 Garmisch Partenkirchen, Germany. (martin.misslbeck@imk.fzk.de; stephan.thiel@imk.fzk.de)

R. Schmitt, Meteorologie Consult GmbH, Frankfurterstrasse 28, D-61462 Kinogstein, Germany. (metcon@metcon-us.com)